Geology
March 2014, Volume 42, Issue 3, Pages 183-186
http://dx.doi.org/10.1130/G35070.1

Land-ocean changes on orbital and millennial time scales and the penultimate glaciation

Vasiliki Margari[1], Luke C. Skinner[2], David A. Hodell[2], Belen Martrat[3], Samuel Toucanne[4], Joan O. Grimalt[3], Philip L. Gibbard[5], J.P. Lunkka[6] and P.C. Tzedakis[1]

[1] Environmental Change Research Centre, Department of Geography, University College London, London WC1E 6BT, UK
[2] Department of Earth Sciences, University of Cambridge, Cambridge CB2 3EQ, UK
[3] Institute of Environmental Assessment and Water Research (IDAEA), Spanish Council for Scientific Research (CSIC), 08034 Barcelona, Spain
[4] IFREMER, Laboratoire Environnements Sédimentaires, F-29280 Plouzané, France
[5] Department of Geography, University of Cambridge, Cambridge CB2 3EN, UK
[6] Institute of Geosciences, University of Oulu, Oulu, FIN-90014, Finland

Abstract:

Past glacials can be thought of as natural experiments in which variations in boundary conditions influenced the character of climate change. However, beyond the last glacial, an integrated view of orbital- and millennial-scale changes and their relation to the record of glaciation has been lacking. Here, we present a detailed record of variations in the land-ocean system from the Portuguese margin during the penultimate glacial and place it within the framework of ice-volume changes, with particular reference to European ice-sheet dynamics. The interaction of orbital- and millennial-scale variability divides the glacial into an early part with warmer and wetter overall conditions and prominent climate oscillations, a transitional mid-part, and a late part with more subdued changes as the system entered a maximum glacial state. The most extreme event occurred in the mid-part and was associated with melting of the extensive European ice sheet and maximum discharge from the Fleuve Manche river. This led to disruption of the meridional overturning circulation, but not a major activation of the bipolar seesaw. In addition to stadial duration, magnitude of freshwater forcing, and background climate, the evidence also points to the influence of the location of freshwater discharges on the extent of interhemispheric heat transport.

1. Introduction

The penultimate glacial (~135–185 ka) corresponds to Marine Isotope Stage (MIS) 6, the Illinoian glaciation in North America and the late Saalian glaciation in Europe. The latter was characterized by two major ice advances, the more extensive Drenthe followed by the Warthe (Ehlers et al., 2011). During Marine Isotope Substage 6e (*sensu* Margari et al., 2010) ~165–179 ka, boreal summer insolation reached interglacial values and was accompanied by an intensification of monsoonal systems (Wang et al., 2008), deposition of sapropel layer S6 and pluvial conditions in the Mediterranean (Bard et al., 2002), while sea-level was –40 to –60 m relative to present (Thompson and Goldstein, 2006). In terms of millennial-scale changes, low detrital carbonate content at several North Atlantic sites (e.g. McManus et al., 1999; de Abreu et al., 2003; Hemming, 2004; Channell et al., 2012) suggests that iceberg discharges through Hudson Strait were reduced compared to other glacials. Despite the absence of typical Heinrich events, stadial conditions persisted longer during the first part of MIS6 than comparable non- Heinrich stadials in MIS3, reflecting the influence of background climate on MOC strength (Margari et al., 2010). Regarding terrestrial changes, apart from a few exceptions (e.g. Wang et al., 2008; Roucoux et al., 2011), there is a dearth of high-resolution records spanning MIS6. Here we return to the Portuguese margin and examine land-ocean changes during MIS6 and their relation to the record of glaciation.

SETTING AND EARLIER WORK

Previous work on the Portuguese margin has highlighted its importance for tracing millennial-scale variability and undertaking land-sea comparisons. A key aspect is that the area is located sufficiently near to the continent to derive a regional pollen signal, but deep enough to generate high-quality isotopic records that are pertinent to basin-wide phenomena. During MIS3, the $\delta^{18}O_{planktonic}$ and sea-surface temperature (SST) records closely matched the Greenland $\delta^{18}O_{ice}$ sequence, while the $\delta^{18}O_{benthic}$ curve resembled the temperature curve from Antarctica, both in its shape and phasing relative to changes in $d^{18}O_{planktonic}$ (Shackleton et al., 2000; Martrat et al., 2007; Skinner et al., 2007). Concerning land-sea comparisons, joint pollen and foraminiferal isotope analyses have established the immediate response of vegetation to millennial-scale variability (e.g. Sanchez Goñi et al., 2000; Roucoux et al., 2001) and a close coupling of low- and mid-latitude hydrological changes via shifts in the mean latitudinal position of the Intertropical Convergence Zone (ITCZ) (e.g. Tzedakis et al., 2009).

MATERIALS AND METHODS

Core MD01–2444 (37°33.68’N; 10°08.53’W; 2637m water depth; 27.45m long) was recovered from an elevated spur on the continental rise, using the CALYPSO Giant Piston corer aboard the *Marion Dufresne II*. In the MIS6 section of MD01–2444, sediment accumulation rates are ~10cm/kyr. Pollen and stable isotope analyses were undertaken on the same levels every 3 cm; XRF analyses were obtained every 2 mm (see Margari et al. [2010] and Hodell et al. [2013] for methods).

Here, we use the chronology of Barker et al. (2011), based on alignment of SST changes in MD01–2444 to the synthetic Greenland (GL_T-syn) record (Table DR1). GL_T-syn was constructed from the EDC δD record, using the bipolar-seesaw model, and placed on an absolute timeframe by alignment to precisely-dated Chinese speleothems for the interval 0–400 ka (Barker et al., 2011). The placement of the MD01–2444 sequence on the speleothem timescale permits an independent investigation of the phase responses of proxy records relative to orbital forcing.

RESULTS AND DISCUSSION

Millennial-Scale Changes

Millennial-scale variability is pervasive and especially prominent during the first half (160–185 ka) of MIS6 (Fig. 1), with the $\delta^{18}O_{planktonic}$ and $\delta^{18}O_{benthic}$ records showing the same asynchronous phasing as observed during MIS3 by Shackleton et al. (2000), suggesting changes in surface and deep-water hydrography consistent with the operation of the bipolar-seesaw (Margari et al., 2010). The alkenone-based SST reconstructions contain a similar number of oscillations (Martrat et al., 2007), but the overall profile shows relatively small and short-lived SST falls from a baseline of ~15°C, except for a large decrease ~154–157 ka. For most of MIS6 (until ~145 ka), variations in temperate tree pollen percentages (Fig. 1) closely mirror the $\delta^{18}O_{planktonic}$ record, suggesting the synchronous response of vegetation to North Atlantic millennial-scale variability (Margari et al., 2010). During interstadials, arboreal populations (composed primarily of deciduous *Quercus*) expanded, while Mediterranean vegetation communities (mainly evergreen *Quercus*) were present in smaller abundance. During stadials, steppe communities (*Artemisia*, Chenopodiaceae and *Ephedra*) were the dominant vegetation type (Fig. DR1).

The structure of millennial-scale oscillations in MD01–2444 during MIS6e is similar to that seen in speleothems from France and China (Wainer et al., 2013; Wang et al., 2008), suggesting coherent hemispheric changes in climate, as already observed in MIS3. Considering the entire MIS6 interval, we note that the temperate tree pollen record matches the Greenland GL_{T}-syn curve of Barker et al. (2011) more closely than the $\delta^{18}O_{planktonic}$ and the alkenone SST sequences. This may arise from the way the three proxies each record a differently biased or convolved measure of local conditions and how these relate to the bipolar-seesaw, which is the basis of the GL_{T}-syn curve. The fact that vegetation and hydrological changes associated with millennial-scale shifts in the ITCZ (Tzedakis et al., 2009) closely track the GL_{T}-syn record therefore suggests that these processes are more tightly linked to the bipolar-seesaw.

Orbital-Scale Changes

Hodell et al. (2013) have shown that variations in sediment composition in MD01–2444 contain strong precessional power, with the ratio of biogenic (Ca) to detrital (Ti) sediments lagging precession minima by ~7 kyr (Fig. 2). On orbital timescales, Ca/Ti minima in this area reflect dilution of carbonate accumulation by increased clay flux, while on millennial timescales Ca/Ti minima correspond to cold events, reflecting decreases in carbonate productivity (Hodell et al., 2013) and/or increased detrital sedimentation (Lebreiro et al., 2009). In terms of vegetation changes, while variations in temperate tree populations are dominated by millennial-scale variability, other taxon-specific responses show a clear precessional cyclicity superimposed on millennial oscillations. Most striking is the Ericaceae (heathland) curve with three major expansions coinciding with perihelion passage in winter (Fig. 2). The expansion of Ericaceae during intervals of minimum boreal summer insolation and reduced seasonality reflects reduced summer aridity and greater annual moisture availability (Margari et al., 2007; Fletcher and

Sánchez Goñi, 2008), associated with the southernmost latitudinal summer position of the ITCZ. The Ericaceae percentages closely covary with changes in the Ca/Ti record, which may point to a causal mechanism whereby expanded vegetation cover during times of moisture availability prevented increased erosion and discharge of detrital material by the Tagus river. Alternatively, the Ca/Ti and Ericaceae signals may represent independent but synchronous responses to climate forcing.

Integration with the Record of Glaciation

Global sea-level reconstructions (Thompson and Goldstein, 2006; Elderfield et al., 2012) indicate a sea-level fall after ~163 ka, likely associated with a rapid advance of the Drenthe ice-sheet to its maximum extent (Fig. 3). This was followed by ice-sheet melting under increasing summer insolation and a sea-level rise ~157 ka. The most extreme conditions occurred at ~157–154 ka, characterized by coldest SSTs, minimum $\delta^{13}C_{benthic}$ values and a collapse of moisture-requiring temperate tree and Ericaceae populations (Fig. 3). This event appears coeval with large seasonal discharges of the Fleuve Manche river (Channel River), indicated by thick laminated facies and peaks in freshwater algae in the Bay of Biscay (Eynaud et al., 2007), originating from the rapid wasting of the Drenthe ice-sheet (Toucanne et al., 2009). The correlation is also supported by maximum values in the relative proportion of tetra-unsaturated alkenones ($C_{37:4}$%) in MD01–2444, which could reflect the advection of cold surface water to the Portuguese margin (Martrat et al., 2007). However, this mid-MIS6 event (Fig. 1) is only accompanied by subdued asymmetric phasing in planktonic-benthic $\delta^{18}O$ and a particularly slow warming in Antarctica, suggesting a weak impact on interhemispheric heat transport, despite its stadial duration (3 kyr) in the North Atlantic (cf. EPICA Community Members, 2006). An analogy has been drawn with another episode of strong Fleuve Manche discharge during Heinrich Stadial (HS) 1 (~17 ka)

(Toucanne et al., 2009), but HS1 was characterized by Hudson Strait derived detrital carbonate (e.g. Hemming, 2004) and was coeval with warming in Antarctica. Earlier (but less extreme) Fleuve Manche discharges at ~270 and ~340 ka (Toucanne et al., 2009) were also associated with Hudson Strait discharges (Channell et al., 2012) and warming in Antarctica (Jouzel et al., 2012). By contrast, the absence of detrital carbonate in North Atlantic sediments during the mid-MIS6 event (Channell et al., 2012) points to reduced Hudson Strait discharges. The lack of major bipolar-seesaw activity at that time could therefore be related to the origin of freshwater discharge into the North Atlantic, which may have been predominantly European.

No major interstadial warming is indicated by the pollen and planktonic $\delta^{18}O$ records of MD01–2444 during the small summer insolation maximum at 151 ka and this is in concert with the lack of organic deposits and absence of paleosols in northern Europe during the interval between the Drenthe and the Warthe Stadials (Ehlers et al., 2011). After ~150 ka, eustatic sea level records and glacial geological evidence suggest that ice-sheets expanded, with global ice-volume reaching its maximum extent towards the end of MIS6, reflecting the growth of the late Illinoian ice-sheet in North America (e.g. Curry et al., 2011; Syverson and Colgan, 2011). In Europe, the Warthe I and II ice advances were less extensive than the Drenthe (Ehlers et al., 2011), but that may have been compensated for by ice expansion in Russia and Siberia (e.g. Astakhov, 2004). Compared to the last glacial maximum, late MIS6 was characterized by overall larger ice-sheets, supporting the view that the strongest glacials occur when the system skips a small insolation maximum, with limited ice loss, and continues its trajectory towards increasingly colder conditions (Raymo, 1997; Paillard, 2001).

EMERGING PATTERNS

Taken together, the records of changes in the land-ocean system from the Portuguese margin form a coherent framework with the evidence of ice-volume variations during MIS6. On the basis of the amplitude of millennial-scale variability, the penultimate glacial may be divided into three parts: (i) early (185–160 ka) with prominent oscillations in foraminiferal isotope and tree pollen values; (ii) transitional (160–150 ka); and (iii) late (150–135 ka) with subdued benthic $\delta^{18}O$ and $\delta^{13}C$, and Antarctic δD variations (but with excursions in surface ocean conditions, perhaps associated with Warthe ice movements), and minimum temperate tree pollen values. This is consistent with the observation that mean climate state modulates the amplitude of millennial-scale variability (e.g. McManus et al. 1999; Tzedakis, 2005; Barker et al., 2011). More specifically, the overall warmer and wetter conditions of early MIS6 associated with the strong boreal summer insolation maximum at 175 ka, combined with excess ice of –40 to –60 m sea-level equivalent, were marked by accentuated millennial-scale variability and activation of the bipolar-seesaw. By contrast, the character of changes after 150 ka is consistent with a reduction of millennial variability as climate approached a more stable maximum glacial state, which culminated into one of the largest Quaternary glaciations. However, the muted bipolar-seesaw variability during the mid-MIS6 event was not related to an extreme glacial state, as relative sea level (–35 to –65 m) was within the millennial climate instability window. We suggest that in addition to North Atlantic stadial duration (EPICA Community Members, 2006), magnitude of freshwater forcing (Ganopolski and Rahmstorf, 2001) and background climate (Margari et al., 2010), the regional distribution of ice-sheets and location of freshwater discharge may have also influenced interhemispheric heat transport. Such natural experiments under different boundary conditions provide a more nuanced view of freshwater forcing, MOC sensitivity and global climate.

ACKNOWLEDGMENTS

The study was supported by NERC (NE/C514758/1), EU (EV K2–CT–2000–00089) and the Royal Society. We thank A. Ganopolski for discussions, F. Eynaud for providing the MD03–2692 data and the reviewers and editor for their comments.

REFERENCES CITED

Astakhov, V.I., 2004, Middle Pleistocene glaciations of the Russian North: Quaternary Science Reviews, v. 23, p. 1285–1311, doi:10.1016/j.quascirev.2003.12.011.

Bard, E., Antonioli, F., and Silenzi, S., 2002, Sea-level during the penultimate interglacial period based on a submerged stalagmite from Argentarola Cave (Italy): Earth and Planetary Science Letters, v. 196, p. 135–146, doi:10.1016/S0012-821X(01)00600-8.

Barker, S., Knorr, G., Edwards, L., Parrenin, F., Putnam, A.E., Skinner, L.C., Wolff, E., and Ziegler, M., 2011, 800,000 years of abrupt climate variability: Science, v. 334, p. 347–351, doi:10.1126/science.1203580.

Berger, A., 1978, Long-term variations of caloric insolation resulting from the earth’s orbital elements: Quaternary Research, v. 9, p. 139–167, doi:10.1016/0033-5894(78)90064-9.

Channell, J.E.T., Hodell, D.A., Romero, O., Hillaire-Marcel, C., deVernal, A., Stoner, J.S., Mazaud, A., and Röhl, U., 2012, A 750-kyr detrital-layer stratigraphy for the North Atlantic (IODP Site U1302–U1303, Orphan Knoll, Labrador Sea): Earth and Planetary Science Letters, v. 317–318, p. 218–230, doi:10.1016/j.epsl.2011.11.029.

Curry, B.B., Grimley, D.A., and McKay, E.D., III, 2011, Quaternary glaciations in Illinois, *in* Ehlers, J., Gibbard, P.L., and Hughes, P.D., eds., Quaternary Glaciations - Extent and Chronology - A Closer Look: Developments in Quaternary Science 15, p. 467–487.

de Abreu, L., Shackleton, N.J., Schönfeld, J., Hall, M., and Chapman, M., 2003, Millennial-scale oceanic climate variability off the Western Iberian margin during the last two glacial periods: Marine Geology, v. 196, p. 1–20, doi:10.1016/S0025-3227(03)00046-X.

Ehlers, J., Grube, A., Stephan, H.-J., and Wansa, S., 2011, Pleistocene glaciations of North Germany—New results, *in* Ehlers, J., Gibbard, P.L., and Hughes, P.D., eds., Quaternary Glaciations - Extent and Chronology - A Closer Look: Developments in Quaternary Science 15, p. 149–162.

Elderfield, H., Ferretti, G., Greaves, M., Crowhurst, S., McCave, I.N., Hodell, D., and Piotrowski, A.M., 2012, Evolution of ocean temperature and ice-volume through the Mid-Pleistocene climate transition: Science, v. 337, p. 704–709, doi:10.1126/science.1221294.

EPICA community members, 2006, One-to-one coupling of glacial variability in Greenland and Antarctica: Nature, v. 444, p. 195–198.

Eynaud, F., Zaragosi, S., Scourse, J.D., Mojtahid, M., Bourillet, J.F., Hall, I.R., Penaud, A., Locascio, M., and Reijonen, A., 2007, Deglacial laminated facies on the NW European continental margin: The hydrographic significance of British-Irish Ice Sheet deglaciation and Fleuve Manche paleoriver discharges: Geochemistry Geophysics Geosystems, v. 8, Q06019, doi:10.1029/2006GC001496.

Fletcher, W.J., and Sánchez Goñi, M.F., 2008, Orbital- and sub-orbital-scale climate impacts on vegetation of the western Mediterranean basin over the last 48,000 yr: Quaternary Research, v. 70, p. 451–464, doi:10.1016/j.yqres.2008.07.002.

Ganopolski, A., and Rahmstorf, S., 2001, Rapid changes of glacial climate simulated in a coupled climate model: Nature, v. 409, p. 153–158, doi:10.1038/35051500.

Hemming, S.R., 2004, Heinrich events: Massive late Pleistocene detritus layers of the North Atlantic and their global climate imprint: Reviews of Geophysics, v. 42, RG1005, doi:10.1029/2003RG000128.

Hodell, D., Crowhurst, S., Skinner, L., Tzedakis, P.C., Margari, V., Maclaghlan, S., and Rothwell, G., 2013, Response of Iberian Margin sediments to orbital and suborbital forcing over the past 420 kyr: Paleoceanography, v. 28, p. 1–15, doi:10.1002/palo.20017.

Jouzel, J. and 17 others, 2007, Orbital and millennial Antarctic climate variability over the past 800,000 years: Science, v. 317, p. 793–796, doi: 10.1126/science.1141038.

Lebreiro, S.M., Voelker, A.H.L., Vizcaino, A., Abrantes, F.G., Alt-Epping, U., Jung, S., Thouveny, N., and Gracia, E., 2009, Sediment instability on the Portuguese continental margin under abrupt glacial climate changes (last 60 kyr): Quaternary Science Reviews, v. 28, p. 3211–3223, doi:10.1016/j.quascirev.2009.08.007.

McManus, J.F., Oppo, D.W., and Cullen, J.L., 1999, A 0.5-million-year record of millennial-scale climate variability in the North Atlantic: Science, v. 283, p. 971–975, doi:10.1126/science.283.5404.971.

Margari, V., Tzedakis, P.C., Shackleton, N.J., and Vautravers, M., 2007, Vegetation response in SW Iberia to abrupt climate change during MIS 6: Direct land-sea comparisons: Quaternary International, v. 167–168, Supplement 1, p. 267–268.

Margari, V., Skinner, L.C., Tzedakis, P.C., Ganopolski, A., Vautravers, M., and Shackleton, N.J., 2010, The nature of millennial-scale climate variability during the past two glacial periods: Nature Geoscience, v. 3, p. 127–131, doi:10.1038/ngeo740.

Martrat, B., Grimalt, J.O., Shackleton, N.J., de Abreu, L., Hutterli, M.A., and Stocker, T.F., 2007, Four climatic cycles of recurring deep and surface water destabilizations on the Iberian Margin: Science, v. 317, p. 502–507, doi:10.1126/science.1139994.

Paillard, D., 2001, Glacial cycles: Towards a new paradigm: Reviews of Geophysics, v. 39, p. 325–346, doi:10.1029/2000RG000091.

Raymo, M.E., 1997, The timing of major climate terminations: Paleoceanography, v. 12, p. 577–585, doi:10.1029/97PA01169.

Roucoux, K.H., Tzedakis, P.C., Lawson, I.T., and Margari, V., 2011, Vegetation history of the penultimate glacial period (Marine Isotope Stage 6) at Ioannina, north-west Greece: Journal of Quaternary Science, v. 26, p. 616–626, doi:10.1002/jqs.1483.

Sánchez Goñi, M.F., Turon, J.-L., Eynaud, F., and Gendreau, S., 2000, European climatic response to millennial-scale changes in the atmosphere-ocean system during the last glacial period: Quaternary Research, v. 54, p. 394–403, doi:10.1006/qres.2000.2176.

Shackleton, N.J., Hall, M.A., and Vincent, E., 2000, Phase relationships between millennial-scale events 64,000–24,000 years ago: Paleoceanography, v. 15, p. 565–569, doi:10.1029/2000PA000513.

Skinner, L.C., Elderfield, H., and Hall, M., 2007, Phasing of millennial events and Northeast Atlantic deep-water temperature change since ~ 50 ka BP, *in* Schmittner, A., Chiang, J., and Hemming, S.R., eds., Past and Future Changes of the Ocean's Meridional Overturning Circulation: Mechanisms and Impacts: American Geophysical Union Geophysical Monograph, v. 173, p. 197–208.

Syverson, K.M., and Colgan, P.M., 2011, The Quaternary of Wisconsin: An updated review of stratigraphy, glacial history and landforms, *in* Ehlers, J., Gibbard, P.L., and Hughes, P.D., eds., Quaternary Glaciations - Extent and Chronology - A Closer Look: Developments in Quaternary Science 15, p. 537–552.

Thompson, W.G., and Goldstein, S.L., 2006, A radiometric calibration of the SPECMAP timescale: Quaternary Science Reviews, v. 25, p. 3207–3215, doi:10.1016/j.quascirev.2006.02.007.

Toucanne, S., Zaragosi, S., Bourillet, J.F., Cremer, M., Eynaud, F., Van Vliet-Lanoë, B., Penaud, A., Fontanier, C., Turon, J.L., Cortijo, E., and Gibbard, P.L., 2009, Timing of 'Fleuve Manche' discharges over the last 350 kyr: insights into the European ice-sheet oscillations and the European drainage network from MIS 10 to 2: Quaternary Science Reviews, v. 28, p. 1238–1256, doi:10.1016/j.quascirev.2009.01.006.

Tzedakis, P.C., 2005, Towards an understanding of the response of southern European vegetation to orbital and suborbital climate variability: Quaternary Science Reviews, v. 24, p. 1585–1599, doi:10.1016/j.quascirev.2004.11.012.

Tzedakis, P.C., Pälike, H., Roucoux, K.H., and de Abreu, L., 2009, Atmospheric methane, southern European vegetation and low-mid latitude links on orbital and millennial timescales: Earth and Planetary Science Letters, v. 277, p. 307–317, doi:10.1016/j.epsl.2008.10.027.

Wainer, K., Genty, D., Blamart, D., Bar-Matthews, M., Quinif, Y., and Plagnes, V., 2013, Millennial climatic instability during penultimate glacial period recorded on a south-western France speleothem: Palaeogeography, Palaeoclimatology, Palaeoecology, v. 376, p. 122–131, doi:10.1016/j.palaeo.2013.02.026.

Wang, Y.J., Cheng, H., Edwards, R.L., Kong, X.G., Shao, X., Chen, S., Wu, J.Y., Jiang, X.Y., Wang, X.F., and An, Z.S., 2008, Millennial- and orbital-scale changes in the East Asian monsoon over the past 224,000 years: Nature, v. 451, p. 1090–1093, doi:10.1038/nature06692.

FIGURE CAPTIONS

Figure 1. Millennial-scale variations over the interval 135–185 ka. A: $\delta^{18}O$ composition of speleothem calcite from Sanbao Cave, China (Wang et al., 2008). B: Reconstructed $\delta^{18}O$ composition of ice in Greenland synthetic (GL_T-syn) record (Barker et al., 2011). C: MD01–2444 temperate tree pollen (sum of Mediterranean and Eurosiberian taxa, excluding pioneer taxa) percentages. D: MD01–2444 alkenone sea surface temperatures (SST). E: MD01–2444 $\delta^{18}O$ composition of planktonic foraminifera. F: MD01–2444 $\delta^{18}O$ composition of benthic foraminifera. G: Reconstructed δD composition of ice in the EPICA Dome C (EDC) ice core, Antarctica (Jouzel et al., 2007) by Barker et al. (2011). All records are on the Barker et al. (2011) timescale.

Figure 2. Orbital-scale variations over the interval 135–185 ka. A: 21 June insolation for 65°N (Berger, 1978). B: MD01–2444 Ca/Ti ratio. C: MD01–2444 Ericaceae pollen percentages. Shaded intervals denote perihelion passage in winter.

Figure 3. Figure 3. Land-ocean changes from Portuguese margin within the framework of ice-volume variations during the penultimate glacial. A: 21 June insolation for 65°N (Berger, 1978). B: Schematic ice extent in northwestern Europe. C: Sea-level determinations from corals (Thompson and Goldstein, 2006) (diamonds) and deconvolved $\delta^{18}O$ of seawater (Elderfield et al., 2012) (continuous curve). D: Concentration of freshwater alga *Pediastrum* and number of laminations per cm in core MD03–2692 in the Bay of Biscay (Eynaud et al., 2007; Toucanne et al., 2009). E: relative proportion of tetra-unsaturated alkenone ($C_{37:4}$%). F: MD01–2444 $\delta^{13}C$ composition of epifaunal benthic foraminifer *Cibicides wuellestorfi*. G: MD01–2444 alkenone

sea surface temperatures. H: MD01–2444 combined temperate tree and Ericaceae pollen percentages. Timescale of MD03–2692 based on alignment of its *N. pachyderma* (s) abundance record to the alkenone SST curve of MD01–2444 (Figure DR2).

[1]GSA Data Repository items 2014xxx, Table DR1 and Figures DR1 and DR2 are available online at www.geosociety.org/pubs/ft2014.htm, or on request from editing@geosociety.org or Documents Secretary, GSA, P.O. Box 9140, Boulder, CO 80301, USA.

Figure 1

Click here to download Figure: G35070_Fig1.pdf

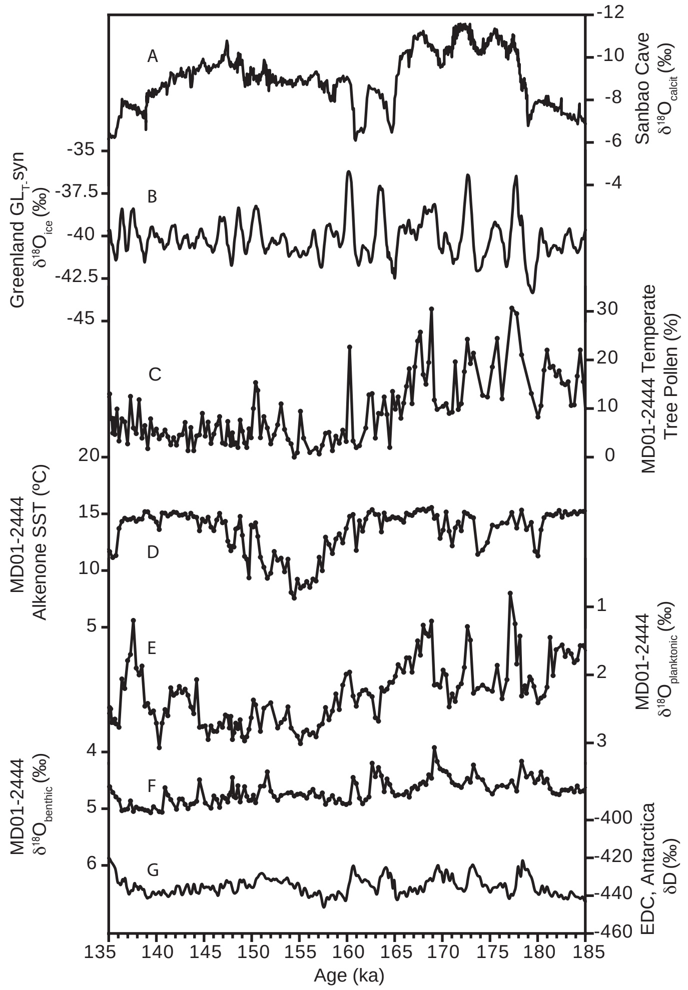

Figure 2
Click here to download Figure: G35070_Fig 2.pdf

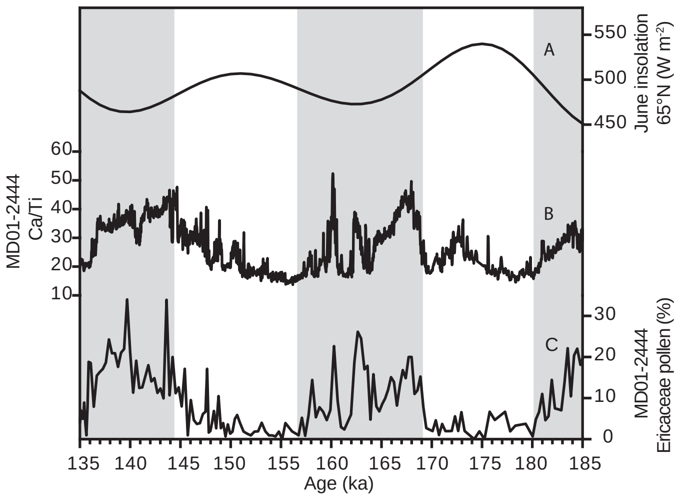

Figure 3

Click here to download Figure: G35070_Fig3.pdf

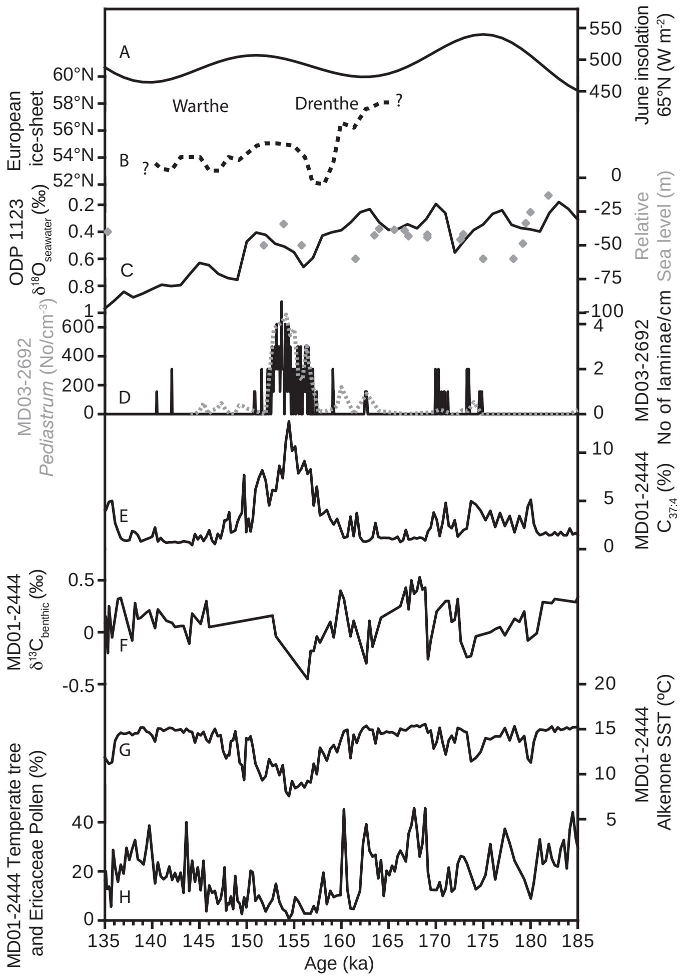

Table DR1. Control points used in the MD01–2444 age model (after Barker et al., 2011*).

Depth (m)	Age (ka)
22.01	135.977
23.15	147.439
23.3	148.249
23.42	149.175
23.63	150.796
23.88	153.807
24.23	157.627
24.48	160.637
24.73	163.415
25.36	169.551
25.72	173.372
26.08	179.508
26.99	189.117
27.28	192.359
27.45	193.864

*Barker, S., Knorr, G., Edwards, L., Parrenin, F., Putnam, A.E., Skinner, L.C., Wolff, E., and Ziegler, M., 2011, 800,000 years of abrupt climate variability: Science, v. 334, p. 347–351, doi:10.1126/science.1203580.

Figure DR1. MD01–2444 selected pollen taxa percentages.

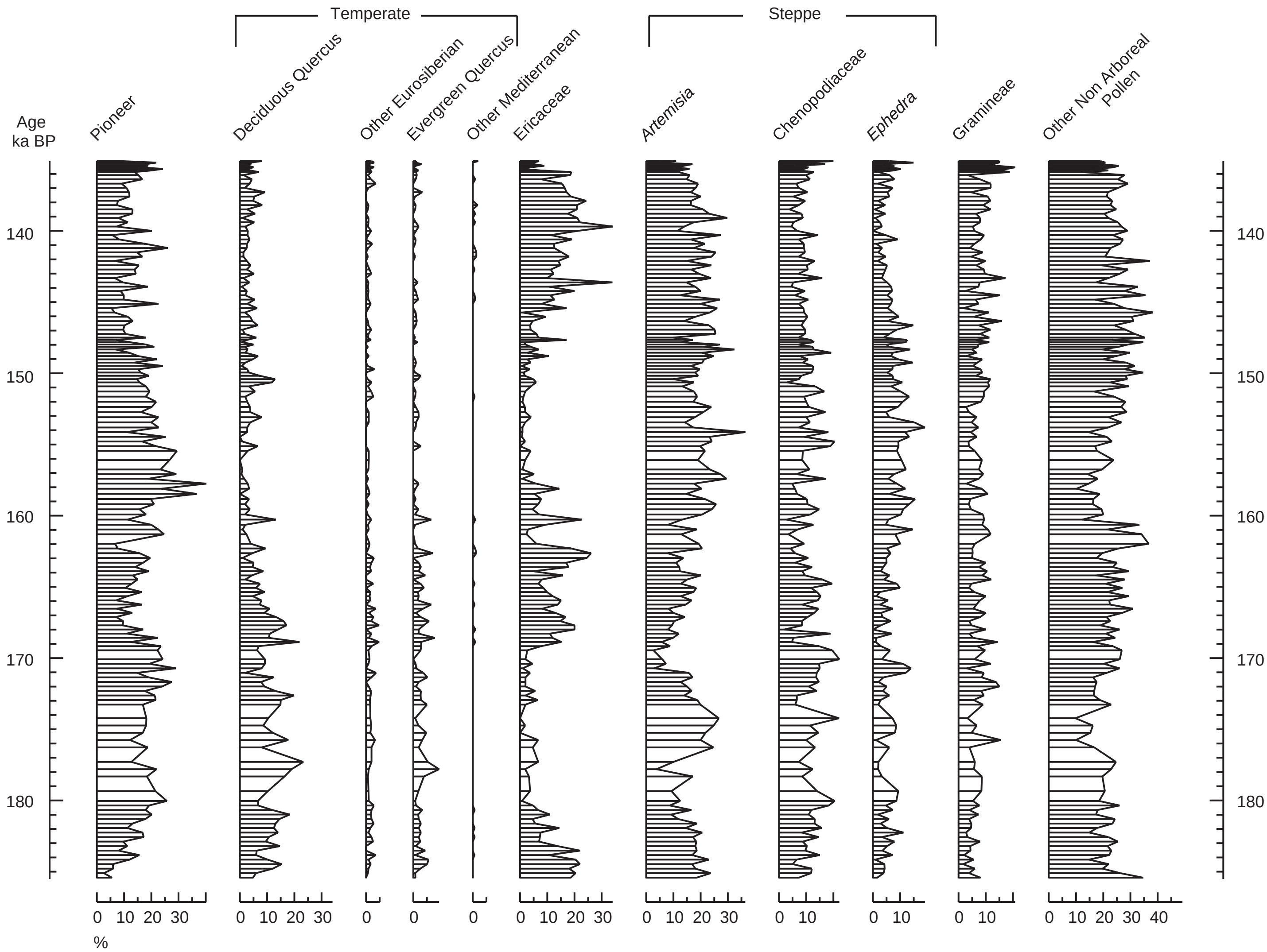

Figure DR2. MD01–2444 selected pollen taxa percentages.